The Abdus Salam
International Centre for Theoretical Physics

United Nations
Educational, Scientific and
Cultural Organization

IAEA
International Atomic Energy Agency

1965-39

9th Workshop on Three-Dimensional Modelling of Seismic Waves Generation, Propagation and their Inversion

22 September - 4 October, 2008

Taiwan and South Island, New Zealand
A Comparison of Continental Collisional Orogenies

Francis T. Wu
Department of Geological Science
State University of New York
Binghamton
New York
USA

francis@binghamton.edu

Taiwan and South Island, New Zealand— A Comparison of Continental Collisional Orogenies

The young, active collision zones in Taiwan and South Island, New Zealand, are bracketed by two subduction zones of opposite polarities. Whereas in South Island two fragments of Gondwanaland are colliding with each other, in Taiwan the Luzon Arc collides with the Eurasian continental margin. The relative plate motion between the Philippine Sea and the Eurasian plates in the Taiwan area is about 3 convergence to 1 transcurrent (80 mm/yr to 27 mm/yr), and in South Island the Pacific to Australian plate motion is 1 convergence to 4 transcurrent (10 mm/yr to 38 mm/yr). Geologically, northern and central Taiwan are underlain by continental crust whereas the southern part corresponds to the transition zone between continent and ocean lithospheres. The eastern Coastal Range is separated from the Central Range by the Longitudinal Valley and is formed by a telescoped arc-forearc sequence of the Luzon arc. In South Island, schists dominate the main part of the orogen; rocks from the Australian plate appear mostly in the northwestern part of South Island and in the central part of the collision zone they form a narrow strip west of the plate boundary, the Alpine fault. The aerial strain measured by GPS in Taiwan is about one order of magnitude greater than that in South Island. In the central part of the two orogens seismicity tends to be shallower and less frequent in the high mountain regions than in the lower ranges. In Taiwan, a portion of the Central Range is nearly aseismic. Substantial roots have been built under both orogens and exhibit an asymmetry mirroring the asymmetry of the mountains. In both orogens the fast-direction of the S-splitting measurements follow the geological trends and in both cases the known crustal delays are too small to account for the observed total delays, arguing for a mantle source of anisotropy and coherent deformation of the crust and upper mantle. The along-strike lithospheric variations in both regions make the orogens strongly three-dimensional.

INTRODUCTION

Arc-continent and continent-continent collisions are major processes in the accretion and development of the continental lithosphere, and their study is important for understanding natural hazard and for resource accumulation. Taiwan and South Island, New Zealand, provide complementary examples of such collisions and a comparative study may allow us to understand the processes more fully. The two regions can be viewed as two end member environments of continental collision – broadly, the convergence of island arc lithosphere with a continental margin in the case of Taiwan and the convergence of two established continental crustal plates in the case of South Island (Plate 1). Although both involve oblique convergence, the rates and proportions differ significantly. The strain rate, seismicity and overall deformation in these two tectonic environments collectively reflect these differences.

TITLE
Geophysical Monograph Series XXX
XXXXXXXXXXXXXXXXXXXXXXXXXXX
10.1029/XXXGMXX

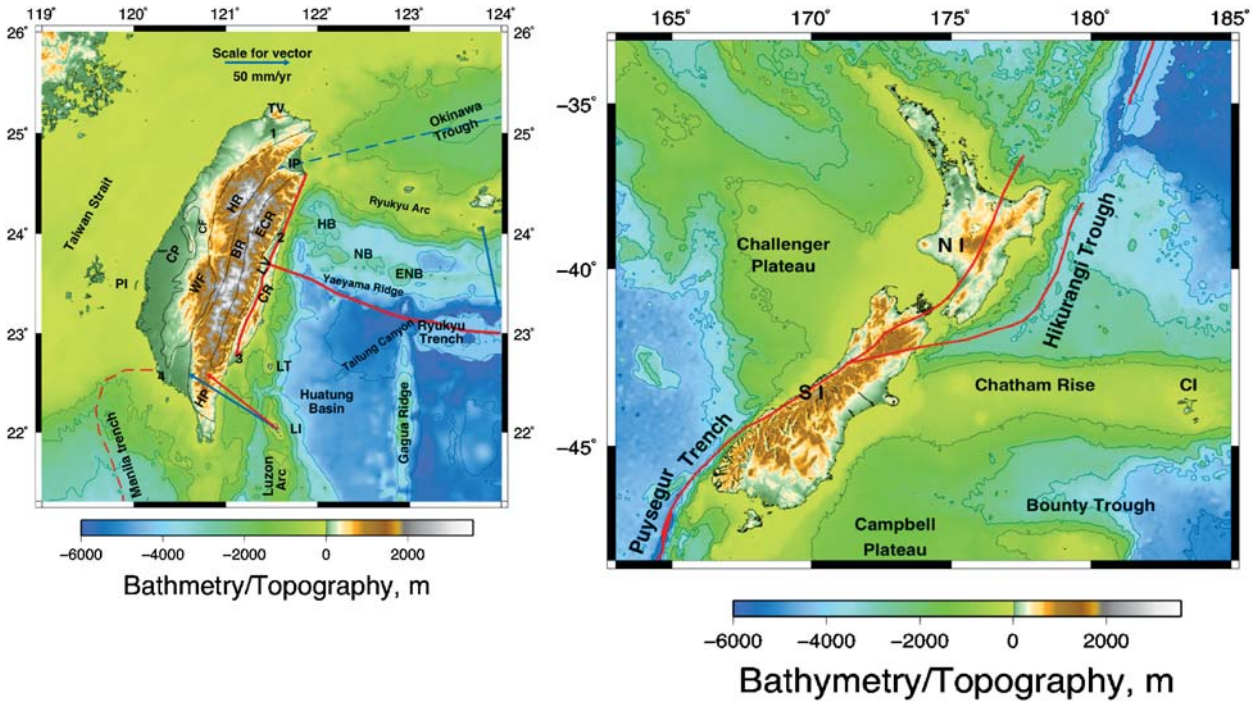

Plate 1. Plate configurations of Taiwan (left) and South Island, New Zealand (right). On the left: The physiographic-geologic units on land are: CR=Coastal Range, ECR=Eastern Central Range, BR=Backbone Range, HR=Hsuehshan Range, WF=Foothills, CP=Coastal Plain, IP=Ilan Plain. CF=Chelungpu fault; TV=Tatun Volcano. LV=Longitudinal Valley. Offshore, HB=Hoping Basin, NB=Nanao Basin, ENB=East Nanao Basin, LI=Lanhsu Island, LT=Lutao Island, and PI=Penghu Islands. Cities, 1=Taipei, 2=Hualian, 3=Taitung. The blue arrows are GPS velocity vectors and the red arrow the NUVEL-1 predicted plate velocity. On the right, CI=Chatham Island, NI=North Island and SI=South Island.

Since this volume contains updated and comprehensive papers on the structure and tectonics of South Island we shall refer to them for most of the basic materials and discussions. This paper will provide materials on Taiwan, some previously published and some new, in order to bring out the contrast and compare the tectonics of the two regions.

In South Island, as detailed by *Davey et al.* [this volume] and *Cox and Sutherland* [this volume] two Gondwanaland continental lithospheric blocks of pre-Cretaceous age but different lithology are colliding. As a result of this collision, the Pacific Plate (PAC) east of the Alpine fault deformed to form the Southern Alps. The Australian Plate (AUS) side, west of the main range, shows little deformation apart from downwarping due to loading by the overthrust Pacific plate. The height of the Southern Alps tapers off slowly toward the north (Marlborough region) and south (Fiordland). The main end member models in this situation relate to how the plate boundary zone evolves - in dip and width - and how the shortening and thickening of the crust and lithospheric mantle are accommodated [*Walcott*, 1998; *Molnar et al.*, 1999].

In Taiwan, the oceanic Luzon island arc embedded in the Philippine Sea plate (PSP) is colliding with the passive continental margin of the Eurasian plate (EUR) (Plate 1). This collision has resulted in the construction of the Central Range on the EUR side and the Coastal Range on the PSP side. Although the main deformation occurs on the island, there have been infrequent M7 or greater events on the Taiwan Strait side to the west and much more frequent M7 or greater events on the PSP side, indicating that the tectonic stresses are high not only under the island but also in its vicinity.

Collisional orogenies such as those in Taiwan and South Island are the primary mechanisms for growth of continents. Much of the Archean and early Proterozoic cratonal consolidation involved the accretion of arc terranes [*Condie*, 2000]. The Paleozoic and early Mesozoic collision of arc complexes results in the tangled record of orogenesis along the Appalachian and Cordilleran margins (e.g., the Taconic, Antler, Sonoma orogenies). Despite the ubiquity of arc-continent collision in the Earth record of continental assembly, most ancient arc-continent collisional events are obscured by later tectonic events, and the plate geometry, plate kinematics, and rates of synorogenic processes are largely unknown. Taiwan and South Island are young, actively forming mountain belts, and the tectonic processes that have been in operation can be readily imaged by geophysical means. While the current seismicity provides information about the stress conditions, the crustal and mantle structures are the integrated effect of orogeny.

Studying the similarities and differences in the plate tectonics that drive these orogenies and the resultant responses of the crust and upper mantle may allow us to better understand how orogenic processes operate. Many questions arise from our study: what are the roles of pure shear and simple deformations in the orogen? How do the different convergence rates affect the style of deformation? Do the orogenies exhibit vertical coherence in the crust and upper mantle? Does the continental plate in the collision subduct? These are among the key questions to be answered not only for these two but for all orogenies. Although we do not yet have complete answers, the seismicity, GPS-based surface deformation, crustal structures and SKS studies of these orogens point toward some possibilities.

GEOLOGIC FRAMEWORK

Taiwan

The Taiwan orogen is built on pre-Tertiary basement with most of the exposed edifice made of Miocene and older rocks. Pliocene and earlier Pleistocene rocks formed deep sedimentary troughs in western Taiwan and some have been folded and faulted to form the western Foothills.

In general, there are seven distinct physiographic and tectonostratigraphic provinces in Taiwan [*Ho*, 1986]. They are shown in the simplified geologic map (Figure 1):

1) the Coastal Plain – the foreland basin,

2) the Western Foothills – the foreland fold-thrust belt in Pliocene-Pleistocene rocks,

3) the Hsuehshan Range – a mountain range built from Eocene-Miocene rocks on the continental shelf,

4) the Central Range – including the metamorphosed Tertiary shelf-slope sediments and the pre-Tertiary metamorphic core,

5) the Longitudinal Valley – a basin that overlies the boundary between continental and arc crust,

6) the Coastal Range – the telescoped Luzon arc complex, trench-forearc complex capped by Miocene andesites, and

7) the Hengchun Peninsula in the south, overlying an active subduction zone, is located in a zone where collision is just beginning [*Liu et al.*, 1997].

Recent detailed mapping of the offshore regions north and south of Taiwan suggests a continuation of many of the structural and geologic patterns recognized on land [*Huang et al.*, 1992; *Liu et al.*, 1997; *Sibuet and Hsu*, 2004]. North and northeast of Taiwan, the collision zone appears to have subsided below sea level owing to the subduction of the PSP along the Ryukyu Trench and to the backarc spreading in the Okinawa Trough (Plate 1). In the region south of Taiwan, subduction of the South China Sea rather than continental lithosphere results in a submarine accretionary prism [*Reed et al.*, 1992] and an active, rather than inactive, magmatic arc.

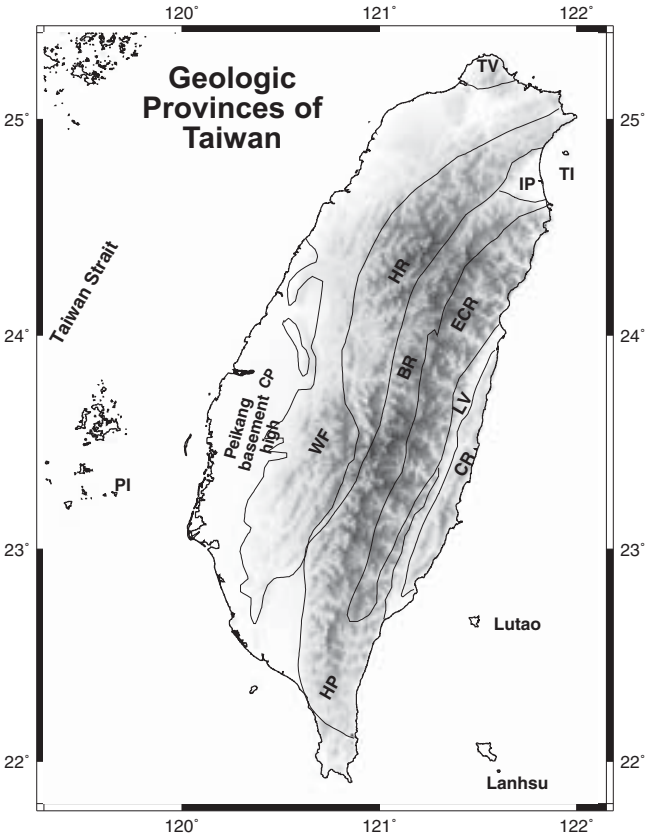

Figure 1. Simplified geologic provinces of Taiwan. Refer to Plate 1 for abbreviations. The additional one is TI=Turtle Island. BR and ECR are often combined and referred to as the Central Range.

South Island

The geology of South Island is generally split into two provinces corresponding largely to the eastern margin of the Australian plate and to the adjacent PAC crust, separated by the Alpine Fault [see Plate 2 in *Cox and Sutherland*, this volume]. West of the Alpine fault, Western Province rocks comprised of Paleozoic metasedimentary and igneous rocks intruded by Cretaceous granitoids form the basement. Western Province rocks are considered to be a fragment of Gondwanaland continental crust [*Cooper*, 1989]. Limited sampling by drillholes shows that similar rocks occur on the offshore Campbell and Challenger plateaus [*Beggs et al.*, 1990; *Wood*, 1991] and at Lord Howe Rise. Eastern Province rocks are a sequence of Mesozoic island arc and metasediments that have been accreted to the Gondwanaland crust. Western Province terranes are separated from those of Eastern Province by the Median Tectonic Zone or the Median Batholith [*Landis and Coombs,* 1967; *Bradshaw*, 1993; *Kimbrough et al.*, 1994; *Mortimer et al.*, 1999; *Tulloch and Kimbrough*, 2003], which records discrete pulses of subduction-related magmatism from about 360 Ma to 105 Ma.

Comparison

In Taiwan the age and metamorphic grade increase eastward towards the Longitudinal Valley, which divides the arc suites from the continental rocks, i.e., the suture; in South Island the grade of metamorphism increases westward toward the plate boundary (the Alpine fault). The folded and faulted Tertiary sediments found in the western Foothills of Taiwan have no corresponding sections in South Island. In Taiwan, thrust faults apparently separate rocks into discrete blocks of common age and grade, but in South Island it is more gradational. The general pattern of foliation changes from west-vergent to east vergent going from west to east across the Central Range of Taiwan as observed by *Lee* [1997]. This pattern is most probably related to the current mode of vertical deformation of the orogen in Taiwan (see later discussion).

The Taiwan orogenic belt is often referred to as a classic example of an arc-continent collision [*Suppe*, 1985; *Twiss and Moores*, 1992; *Davis and Reynolds*, 1996]. Based on mainly surface geology and exploration data down to a few kilometers, a thin-skinned model of mountain building has been proposed to explain the fold-and-thrust belt of the western Foothills [*Davis*, 1983; *Suppe*, 1987] and the detachment was later extended to underlie the whole island [*Carena et al.*, 2002]. In the simplest form of this model a shallow dipping detachment isolates the top layer, where the mountain building is taking place, from the lower layer below, the subducting EUR. Similar models have been used to explain other orogens [*Tozer et al.*, 2002]. But such models are not unique and thick-skinned interpretations of the same orogen have been expounded [e.g., *Coward*, 1996]. In Taiwan, models involving the basement [e.g., *Fuller et al.*, 2006] or lithospheric deformation [*Wu et al.*, 1997] have both been proposed. In South Island, the dominance of the relatively steep Alpine fault in the construction of Southern Alps seems to have ruled out a thin-skinned interpretation. Instead of altered products from processes that have long ceased their actions, here products of ongoing processes can be studied directly, both at the surface and at depth, because Taiwan and South Island are both young and active orogens.

PLATE TECTONIC ENVIRONMENTS

Both Taiwan and South Island lie on a transpressive plate boundary between oppositely dipping subduction zones –

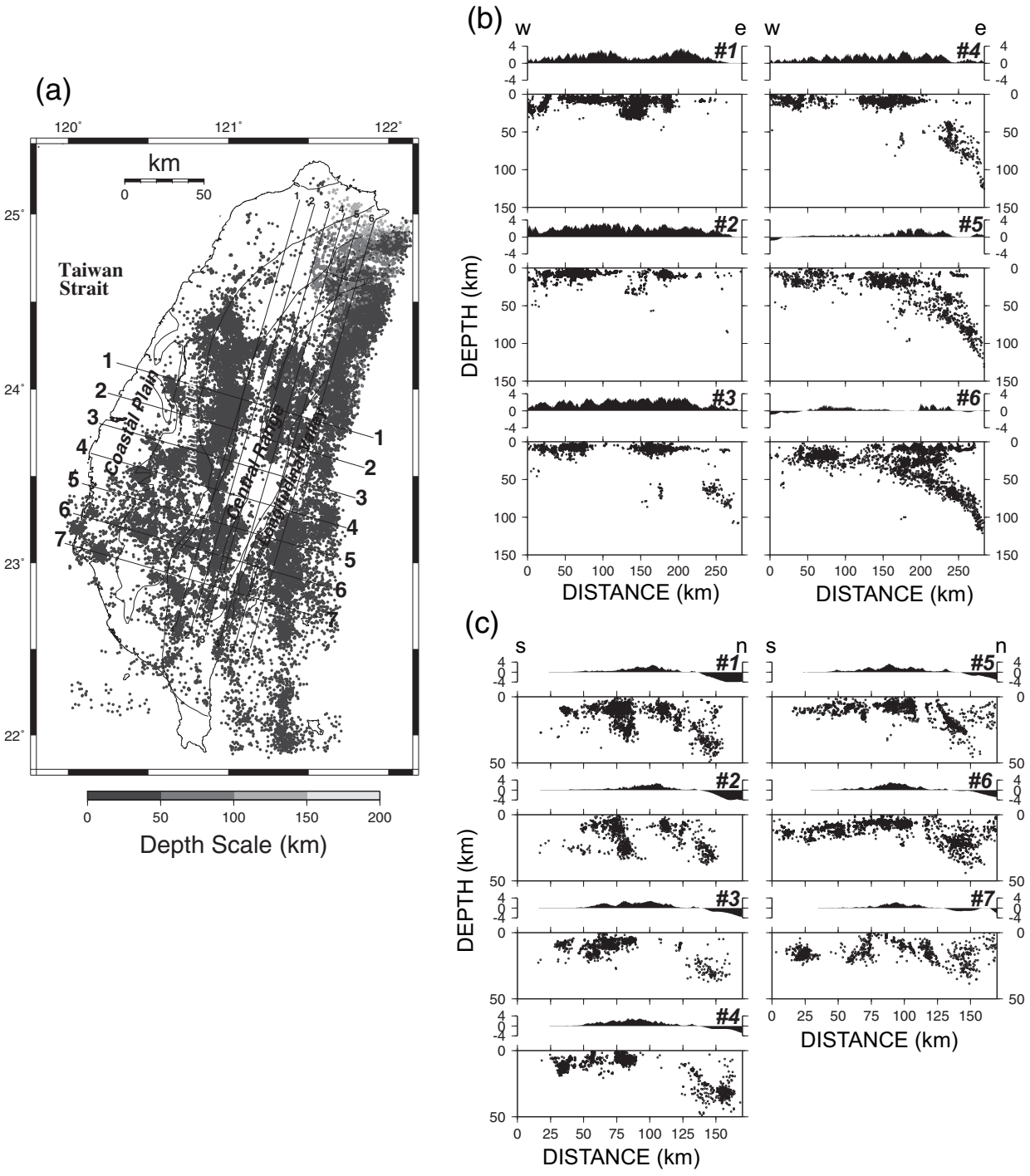

Figure 2. Seismicity in Taiwan (1994–1999). (a) Map view of seismicity and locations of two sets (NNW or N16°E and ESE or S74°E) of profiles. The NNE profiles are nearly in the dip-direction of the Benioff zone. (b) NNE profiles along the trend of the island. (c) ESE profiles perpendicular to the trend of Taiwan. See Plate A1 on the CD-ROM which accompanies this volume, where the map (a) is shown in color. Additionally Figures A1 and A2 on the CD-ROM show the same profiles as in (b) and (c) with the addition of focal mechanisms.

NW-dipping subduction in the north and east dipping subduction in the south (Plate 1). However, there are several significant differences. South Island is about four times the size of Taiwan. The geometry of the colliding plates and rates of convergence are significantly different. The relative plate motion between PSP and EUR in the Taiwan area is about 3 convergence to 1 transcurrent (80 mm/yr to 27 mm/yr), whereas in South Island the PAC to AUS plate motion is 1 convergence to 4 transcurrent (10 mm/yr to 38 mm/yr). In Taiwan, the Ryuku Island Arc and backarc lie at +90° to the continental collision suture (Longitudinal Valley or LV) whereas in South Island the Hikurangi Trench is at +20° to the Alpine fault trend. The Luzon subduction is at –15° to the LV compared to the Puysegur/Fiordland subduction at −30° to Alpine Fault. In other words, subduction zones in South Island can be considered subparallel to the strike of the orogen but the northern subduction zone in Taiwan is perpendicular to the trend of the structures.

The seismicity in these regions illustrate the plate structures quite well because the subduction and collision are very active. We have relocated the seismicity in Taiwan using the double difference technique [*Waldhauser*, 2001]; maps and sections are shown in Figure 2 and also a map of seismicity in color in Plate A1 on the CD-ROM which accompanies this volume. The geometry of the PSP under northern Taiwan can be constructed from the sections in Figure 2b. For comparison with South Island, 3-D animation movies (Animations A1 and A2) and java interactive displays (Animation A3 "Live3D") are included on the CD-ROM which accompanies this volume. In the Live3D display a comparison of the two can be viewed at any angle and can be expanded to show details.

Wu et al. [1997, 2004], among others, interpreted the seismicity in terms of the tectonics of Taiwan; that of South Island has been summarized by *Davey et al.* [this volume]. In the rest of this section we will compare the seismicity of the two regions as related to subduction and discuss the shallow seismicity in central Taiwan later.

Taiwan

Figure 2b shows clearly that under Taiwan the Ryukyu Benioff zone is a well-defined northward dipping zone (Figure 2b, profile #6; see Figure 2a for the location of profiles). However 20 km inland the deeper (>50 km) seismicity is disconnected from the shallow crustal seismicity (Figure 2b, #4). Further inland the deeper seismicity disappears altogether leaving only crustal events (Figure 2b, #2 and #1). Relative to Taiwan, the PSP is moving northwestward at a rate of more than 8 cm/yr and its NNE component causes the PSP to subduct along the westward extension of the Ryukyu Trench (Plate 1). The configuration of the dipping subduction/collision zone implies that the collision boundary of the PSP with EUR varies along the strike of the collisional boundary. North of the junction of the Ryukyu Arc with Taiwan the collision occurs at increasing depth. Although the Ryukyu Trench bathymetric low near Taiwan (Plate 1) is absent, the location of the subduction boundary of the PSP can best be determined using the shape of Benioff zone. As shown in Figure 2b (#6) the Benioff zone begins to bend at about km 130 along the distance axis, corresponding to about 23.7°N. Thus south of 23.7°N the PSP and the EUR are in collision from the surface through the base of the lithosphere but north of this latitude the collision occurs at increasing depths, following the increasing depth of the Benioff zone [*Wu et al.*, 1997, 2007]. With the spreading the Okinawa Trough [*Sibuet et al.*, 1995] the Ryukyu arc moves southward, at a rate of ~60 mm/yr with respect to Taiwan (Plate 1) and the junction of Ryukyu arc with Taiwan will therefore migrate at that rate as well.

The disconnected Benioff zone inland (profile #3 in Figure 2b) probably indicates that as the PSP enters the asthenosphere it can overcome the resistance and move westward. The geometry of the plate edge can be seen more directly in Animations A1, A2 or A3 (Live3D display) on the CD-ROM which accompanies this volume. In Figure A1 and A2 on the CD-ROM we also show the focal mechanisms of M>4.7 events derived from the broadband seismic network (BATS) in Taiwan [*Kao and Jian*, 2001]. For the deeper part of the Benioff zone (>50 km), the down-dip T-axes and horizontal and slab-parallel P-axes dominate, the latter probably related to the continuous push by the PSP westward and the resistence provided by the viscous mantle. The Ryukyu subduction zone has also been imaged as a high velocity anomaly [*Rau and Wu*, 1995; *Kim et al.*, 2005].

The east-dipping seismic zone under the southern tip of Taiwan can be recognized easily from catalog seismicity [*Wu et al.*, 1997]. The double-difference relocation of hypocenters is not effective in the south because the spatial coverage of the land-based network is poor for most of the events, especially the deeper ones to the east of the Hengchun Peninsula. However, the active subduction tectonics of southernmost Taiwan are illustrated by a series of events offshore of western Hengchun at the end of 2006 and the beginning of 2007. Based on world-wide data (Harvard CMT Catalog) the first mainshock of the series has a M_W of 7.0 and centroid depth of 22.5 km (21.83°N, 120.39°E); the normal faulting mechanism has NNW-trending planes. Judging from the crustal structure of the area determined by *McIntosh et al.* [2005] the hypocenter of the earthquake (relocated by *C.S. Chang*, CWB, 2007) places it inside the subducting PSP; similar earthquakes have been observed in many other active subduction zones [*Mikumo et al.*, 2002].

As the Luzon Arc is at an angle with the EUR margin and its collision with the margin created the orogen, a diachronous closing of the ocean basin apparently took place [*Suppe*, 1987]. The Hengchun Peninsula is often considered to be the continuation of the southward propagating Central Range. However, the Coastal Range compressed together the Luzon arc volcanics, the forearc sediments, trench sediments and the volcanic arc (Lutao and Lanhsu – see Figure 1) while just south of the Coastal Range the Manila Trench (the plate boundary west of Hengchun in Plate 1) and the Luzon arc (Lanhsu and Lutao, see Figure 1) are separated by a distance of over 100 km. This implies a discontinuity of the southward propagation of orogeny. That is to say, that south of the latitude of Lutao the collision has barely started while to the north it is a mature collision zone.

Comparison

In South Island, the plate tectonic environment is not as complex, yet is similarly dynamic. Here the plate boundaries and the trend of the orogen are sub-parallel. In addition, the angle between the relative plate motions and the plate boundaries is small however, similar to Taiwan, the main zone of collision is located between the ends of the two subduction zones. Since the southern end of the Hikurangi Trench is known to have been further north than it is at present, the collision section extended farther north than at present. Thus the Marlborough region was within the continental collision zone a few million years ago [*Cox and Sutherland*, this volume].

For both Taiwan and South Island noticeable topography or a sedimentary basin, or both, are found near the junction of the subduction and the collision zones. These tectonophysiological and sedimentological features are related to the geometry and dynamics of the plates. We refer to the steep NE coast of Taiwan and to the west coast of Fiordland and the Seaward Kaikoura Ranges of southwest and northeast South Island, respectively. *Eberhart-Phillips and Reyners* [1997] present 3D velocity images for the latter region derived from the tomographic inversion of earthquake data. In the uppermost mantle they image a low-velocity zone associated with seismicity. They infer this to be related to the continental nature of the subducted plate with the increase in the amplitude of the velocity anomaly to the southwest associated with the increasing thickness of the continental crust being subducted. They suggest that subduction is relatively minor and the plate interface may be locked, leading to the intense deformation at the coastal region. As a result of this attempt to subduct buoyant continental crust, the overriding plate has been compressed, leading to the development of the Kaikoura Ranges (Inland and Seaward) with their very sharp onset at the coast. The very steep topography and the presence of a deep offshore sedimentary basin in Taiwan are apparently the result the fact that only the deeper part of EUR is in collision with PSP, causing the upper portion of EUR to be subjected to EW tension and normal faulting (Plate 1).

Volcanism has not played a very prominent role in either Taiwan or South Island. For Taiwan, in addition to the volcanic arc rocks southeast of Taiwan, the Tatun volcanoes in northern Taiwan overlie the tip of the PSP are possibly still active [*Lin et al.*, 2005]. But we note that no andesitic volcanism is found on South Island, either in the Marlborough or in the Fiordland area. The Solander Island, 30 km south of Fiordland, is calc-andesitic dated at 1 m.y. old. In the north, andesitic volcanism starts half way up North Island (Mt. Ruapehu) and continues along the back-arc basin to offshore of northern North Island. Offshore of northern Taiwan, the Okinawa Trough - an active back-arc basin, extends southwestward into the Ilan Plain area of northern Taiwan, with the dormant Turtle Island volcano offshore (Figure 1). The spreading rate of the Okinawa Trough has been estimated to be about 15 mm/yr for the last two million years [*Sibuet and Hsu*, 1995] but the contemporary rate of southward migration of the southwestern Ryukyu Islands from GPS measurements is about 60 mm/yr (Plate 1) [*Nakamura*, 2004], equivalent to 30 mm/yr of bilateral extension. The rate of extension of the back-arc basin north of North Island is about 20 mm/yr.

Taiwan and South Island share several common tectonic environments, such as a proximity to subduction zones of opposite polarities, a transpressive regime and differences in lithospheric properties across the collision boundaries. There are sufficient differences in boundary conditions and in rates that we should see distinct effects in deformation rates measured at the surface, the seismic response and the resulting crustal structures. We shall now turn towards these observations.

TOPOGRAPHY, SURFACE DEFORMATION AND EROSION

Topography

Central South Island comprises five main zones. From the west, the Australian plate side is a narrow coastal plain that is followed by sharp linear slope change that corresponds to the Alpine fault – the expression of the plate boundary at the surface. Moving eastward, a steep slope up the range front to the main divide of the Southern Alps, a broad intermontane plateau and a less steep slope down to the broad outwash plain form the eastern coastal plain (Figure 2, profile (b) in

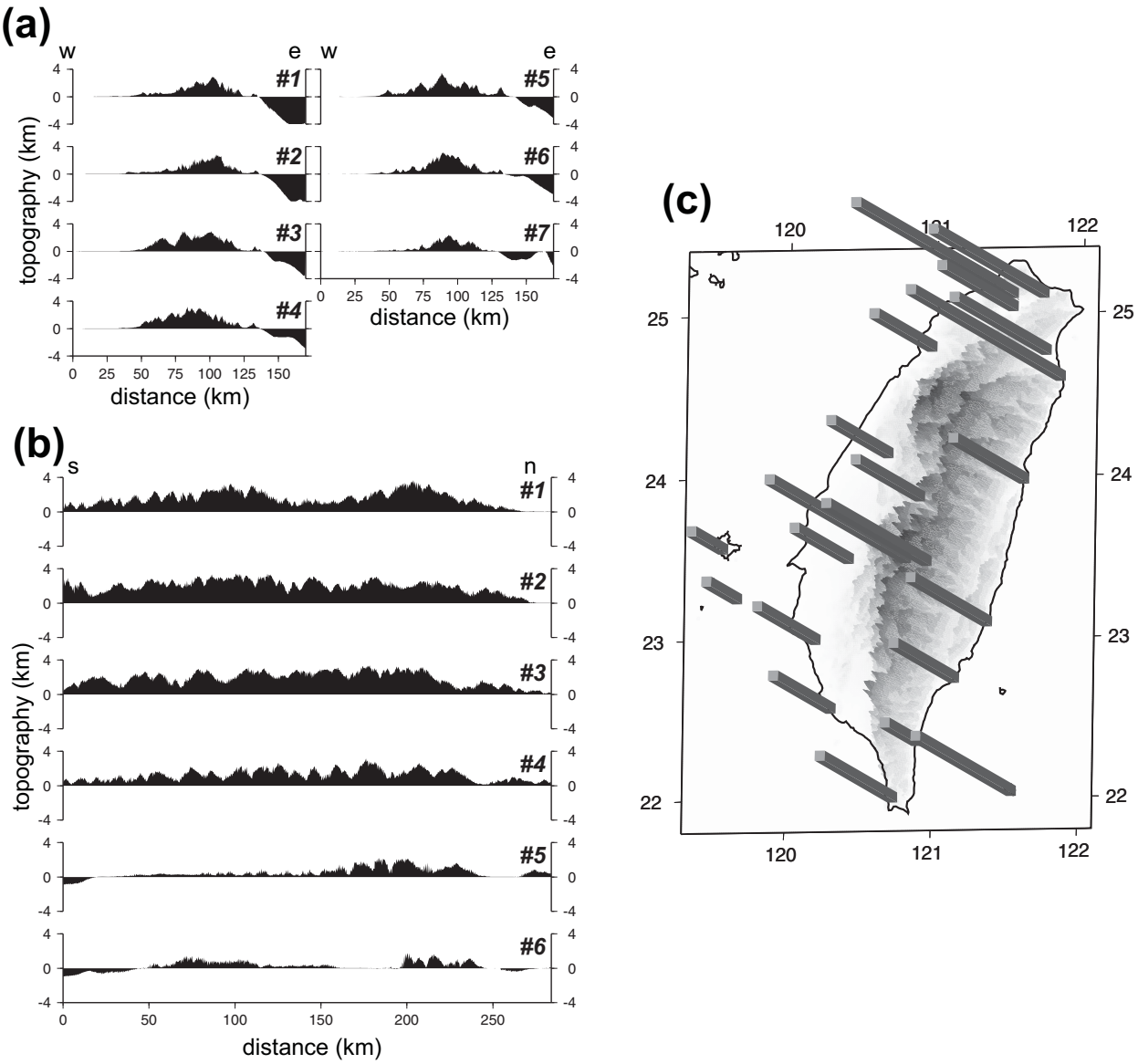

Figure 3. Topography of Taiwan. (a) E-W Profiles perpendicular to the structural trend. Locations same as seismicity profiles in Figure 2b. In southern Taiwan (profiles #6–7), where subduction is taking place, the topography is largely symmetric and in central Taiwan (profiles #1–2), in the collision section, a noted asymmetry is observed. (b) Parallel to the structural trend, locations same as seismicity profiles in Figure 2c. In profile #1, the northern peak is the Hsueshan Range. Profile #3 shows the topography along the axis of the Central Range. (c) 1943–1996 rainfall recorded at cities around the island; the rainfall is proportional to the length of the bar.

Plate 2. (Opposite) Results from the continuous GPS network in Taiwan (L.C. Kuo, IES, Academia Sinica). Arrows show horizontal GPS velocities relative to Penghu Islands and the areal strain rate computed from the velocities using the STRAINSIMPRO326 program from Rick Allmendinger [personal communication, 2007]. The color scale indicates the magnitude of areal strain rate: compression is negative and dilatation is positive. The islands to the southeast of Taiwan sits on the Philippine Sea plate and its velocity can be viewed as the relative velocity between the Philippine Sea plate and the Eurasian plate.

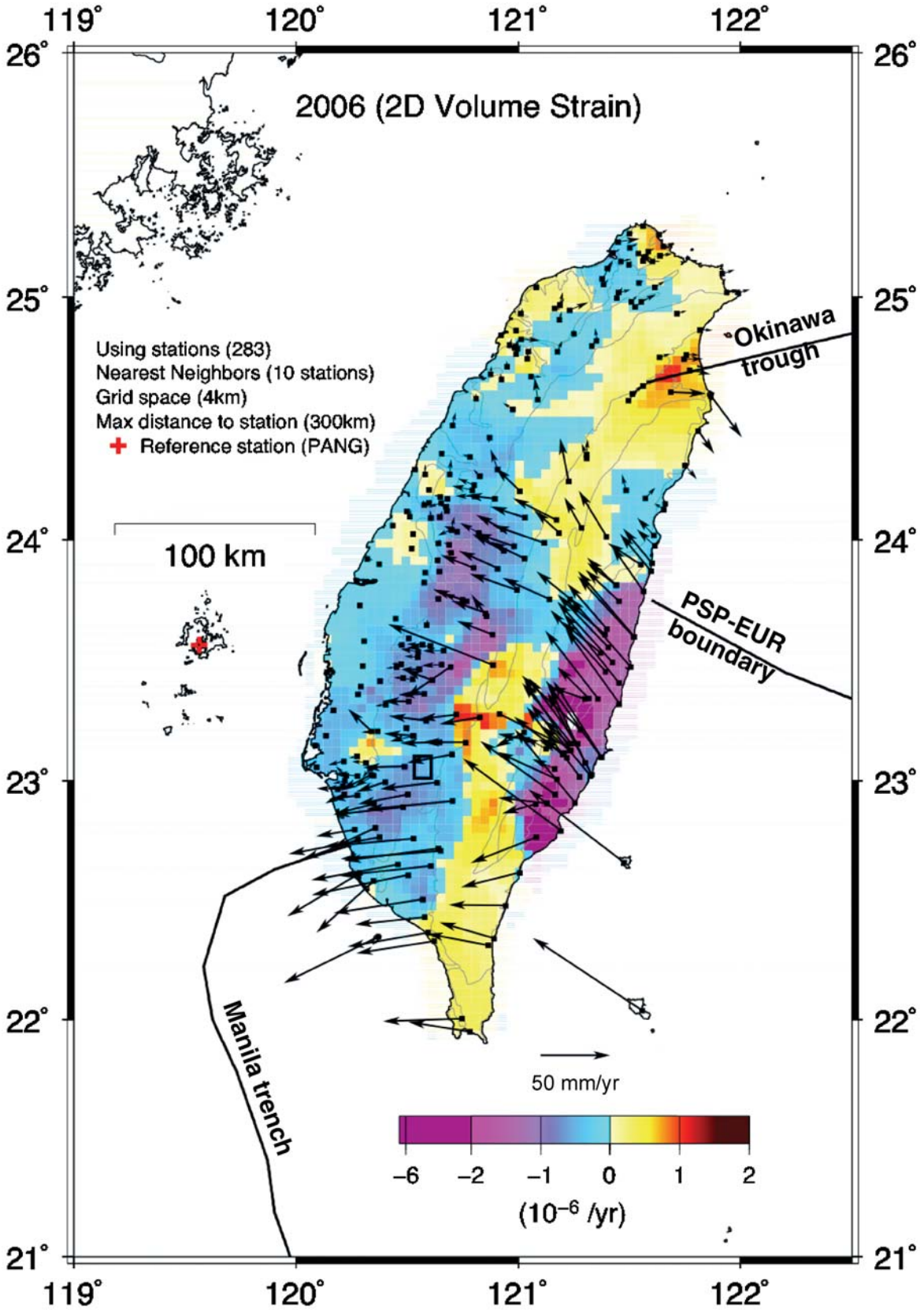
2006 (2D Volume Strain)
119°
120°
121°
122°
26°
25°
24°
23°
22°
21°
Using stations (283)
Nearest Neighbors (10 stations)
Grid space (4km)
Max distance to station (300km)
Reference station (PANG)
100 km
Okinawa trough
PSP-EUR boundary
Manila trench
50 mm/yr
−6
−2
−1
0
1
2
(10−6 /yr)

Davey et al. [this volume]). In the south, a clear orocline turns the trend from NE in central South Island to SE in the Otago region [see *Cox and Sutherland*, this volume].

In central Taiwan, from the PSP side and going west, first the Coastal Range is encountered, reaching a maximum height of approximately 1000 m in the south and 300 m in the north (Figure 3a). The maximum width of the Coastal Range is about 13 km (Figure 1). Across the ~2–3 km wide Longitudinal Valley is the Eastern Central Range. The Coastal Range forms a barrier with only one river from the Central Range flowing across it. The Longitudinal Valley is a long, near sea-level, linear valley that receives sediments while both sides are rising. There is no range-front equivalent of the Alpine fault at the foot of the Central Range side of the Valley, and the rise to the high peaks is not as rapid as the western side of the Southern Alps.

In Taiwan, referring to the physiographic/tectonic provinces mentioned earlier, the highest topography coincides with the Tertiary slates in the Central Range and descends more rapidly on the east side (toward the Longitudinal Valley) than on the west side. In the southwest, the Foothills, formed mainly of sediments deposited on the continental slope and beyond, taper off into the Plain. To the northwest another mountain range, the Hsueshan Range, forms a second topographic high (Figure 3a Profile #3 and Figure 3b Profile #1) and is surrounded by its Foothills and an apron of terraces.

The landforms of both Taiwan and South Island are largely the result of dramatic tectonic deformation and sculpting by erosion. While the deformation process is complex and the subject of current studies, the main agent of erosion is clearly rainfall. As shown in Figure 2 of *Davey et al.* [this volume] the asymmetry of the trend-normal topographic profiles of South Island is very pronounced. It is clear that the orographic rainfall concentrates on the AUS side of the Southern Alps and is the main agent responsible for the erosion [*Batt and Braun*, 1999]. In contrast, Taiwan experiences three types of rainfall: the monsoon from the southwest, the northeastern seasonal rain from the northeast and typhoons that could approach Taiwan from the east, southeast or south. Typhoons are evidently the most powerful erosion mechanism. Rotating moist air masses may hit the rising topography of Taiwan from the east or west, depending on each typhoon's path and may cause heavy rainfall on the windward side of the island. Examples of the rainfall patterns are shown in Plate A2 on the CD-ROM which accompanies this volume. A fair assessment of the cumulative rainfall from typhoons in a few decades is not yet possible. The average rainfall in cities around the island between 1943 and 1996 (Figure 3c) does not show a clear asymmetry. These considerations may point to the fact that an important part of the asymmetry is created by the collisional deformation.

Continuous GPS measurements and deformation

The present rate of deformation is best assessed by campaign or continuous GPS measurements. *Beavan et al.* [this volume] reviewed the GPS data of South Island thoroughly. In Taiwan campaign GPS surveys started in the late 1980's, but a dramatic increase of continuous GPS stations began after the September 20, 1999, Chi-Chi earthquake. *Wu et al.* [2007] have calculated the velocities and strains using the dataset from 2000–2007. Plate 2 shows the velocity vectors, the areal volume strain and the shear strain for 2006. The overall patterns of the year-to-year results do not change but the magnitude of stresses and the rate of deformation rose slowly following the 1999 Chi-Chi earthquake. The large scale patterns of velocity vectors are best explained in terms of plate boundaries, plate motion and deformation. For example, in the central Taiwan collision zone, the velocity vectors gradually decrease from the east coast of Taiwan across the Central Range and the Foothills to very small amplitudes in the Coastal Plain indicating the shortening across the orogen. In the south, the Hengchun Peninsula as a whole is moving at ~40 mm/yr westward with PSP. In contrast, for northern and northeastern Taiwan north of the point where the PSP begins to subduct, a counterclockwise rotation of the vectors, in the area centered around 24°N and 121°E, signifies the end of collision at least in the shallow part of the lithosphere [e.g., *Hu et al.*, 2001] and a decrease in compression. On the other hand, the areal volume strain (Plate 2) shows the relatively high compression in the Coastal Range and the Foothills but a dilatation in most parts of the Central Range. The noise on the vertical component is much higher (~3 mm/yr), and the effect of the 1999 Chi-Chi earthquake prevents us from deciphering the long term trend of the vertical rate at present. In comparison with the results of *Beavan et al.* [this volume], the volume strain is approximately one order of magnitude higher, and the vertical rate is about twice as high. *Lee et al.* [2006] argued that Taiwan was subjected to a two-staged uplift history. From 6 mybp to 1 mybp it rose at a rate of about 1mm/yr and in the last million years it rose at 4–10 mm/yr. If this is the case, then the GPS measurements may be indicating the accelerated deformation.

CRUSTAL AND UPPER MANTLE STRUCTURES

Crustal structures

While detailed crustal seismic data may image deformational structures at a range of scales (e.g., 1–10 km) in an orogen, configuration of the Moho records the cumulative results of the long term deformation, especially if an

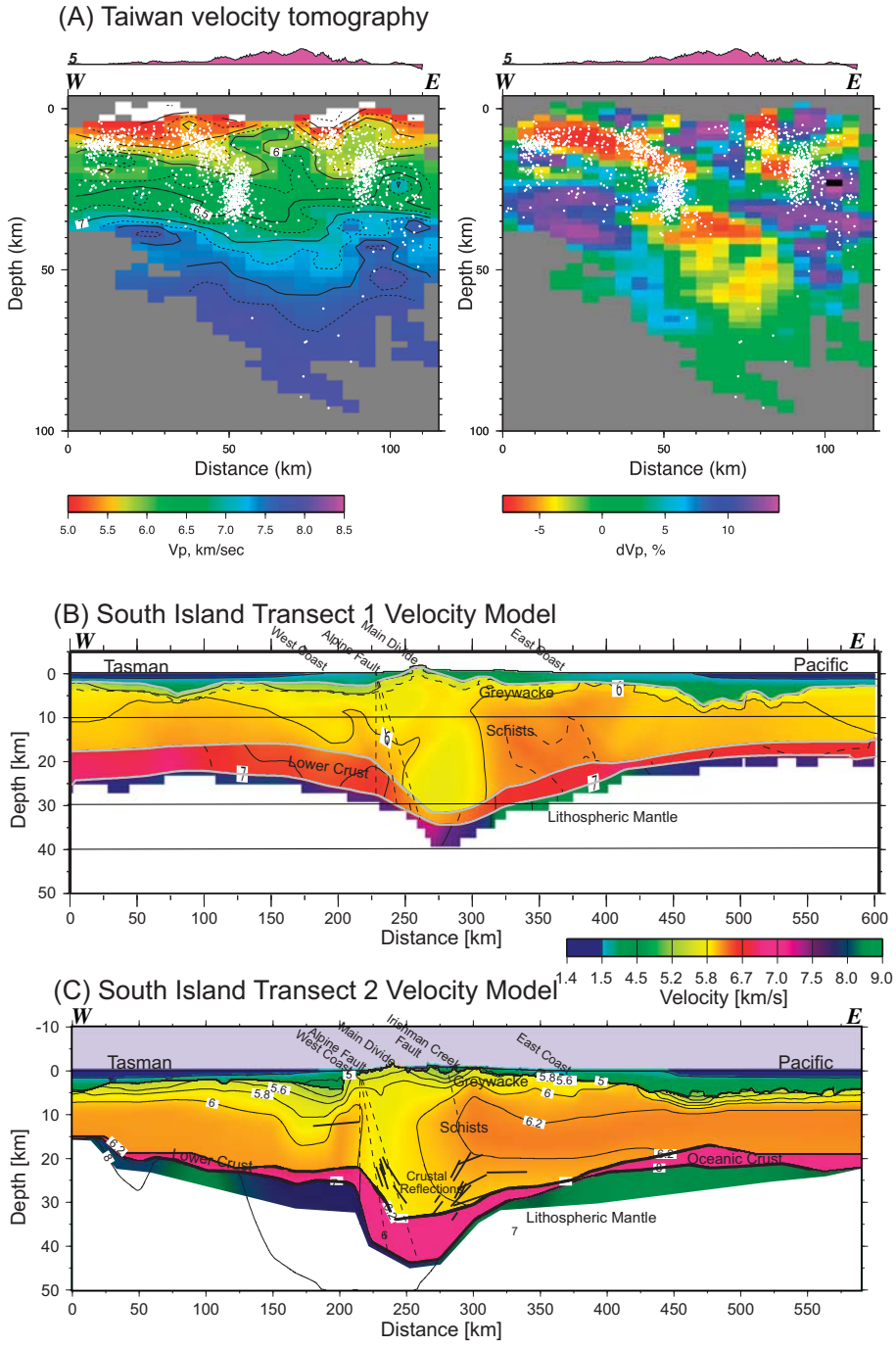

Plate 3. Tomographic section across (a) central Taiwan and (b,c) two transects in central South Island. For (a), cross-sections of Vp (left) and dVp (right), the difference between the final result and the initial model. The white dots are hypocenters of earthquakes. Notice the asymmetry of the crustal root reflecting the topography. If we use the 7.5 km/sec contour as a proxy for Moho, the crustal thickness may exceed 55 km at a distance of about 70 km from the left side of the profile. South Island velocity structures are for Transect 1 (b) and Transect 2 (c) [from *Stern et al.*, this volume].

initial configuration can be assessed. Two key active source transects in South Island (Plate 3b and 3c and also see *Stern et al.* [this volume] and *Davey et al.* [this volume]) show several key features of the crust. Foremost is the presence of a root under the high Southern Alps, noticeably asymmetric with a steeper dipping Moho on the AUS side. We also see the contrast of a gradually thickening crust on the PAC side from the Chatham Rise – Campbell Plateau toward the Southern Alps in both profiles compared to the nearly unchanging Moho depth on the AUS side along Transect 1 (Plate 3b).

Although only limited results from active source work have been obtained in Taiwan so far, crustal images based on local earthquake tomography [*Rau and Wu*, 1995; *Kim et al.*, 2007; *Wu*, 2007] provide a base for comparison. General crustal properties are similar in these studies, represented by a profile across the northern portion of the Central Range (Plate 3a). The profile location is close to Profile #1 in Figure 2b. The earthquakes shown in the profile include the deeper Chi-Chi aftershocks to be discussed in the following seismicity section. The most recently published tomographic result is that of *Wu et al.* [2007], who incorporated a large number of S-P times in the tomography and improved the resolution of Vp/Vs structures.

Using Vp of 7.5 km/s as a proxy for the base of the crust, the crustal thickness of central Taiwan is approximately 55 km, ~10 km thicker than that show in South Islands's transect 2 (Plate 3c). However, the asymmetry is similar with the steep increase of thickness on one side of the colliding plate (PSP in Taiwan and the Australian plate in South Island). A N-S profile in *Rau and Wu* [1995] shows that under the northern tip of the island and in western Taiwan the crust is about 30 km thick; along the spine of the Central Range the base of the crust increases its depth to a maximum depth of 55 km or so as the elevation of the range increases to the north, and then its depth decreases gradually further toward the south.

Mantle Structures

The teleseismic delay times recorded during the SIGHT transect project [*Stern et al.*, 2000, and this volume] were used to identify a high P-wave velocity zone in the upper mantle under South Island. Later, *Kohler and Eberhart-Phillips* [2002] used SAPSE teleseismic delay times for a three-dimensional velocity inversion. They added significant constraints for the exploration of upper mantle structures under South Island. *Davey et al.* [this volume] discuss these results extensively.

Using teleseismic delay times at Taiwan stations [*Chen et al.*, 2004], teleseismic tomography [*Lallemand et al.*, 2001] and combined local earthquake and teleseismic tomography [*Wang et al.*, 2007] a steeply dipping upper mantle high velocity anomaly has been detected. The resolution and velocity contrasts vary in these studies. These anomalies were interpreted to be subducted EUR lithosphere. The zone is not clearly associated with seismicity and this prompted *Lallemand et al.* [2001] to hypothesize a detached lithosphere. Since the collision sections lack significant deep seismicity, the use of high velocity anomalies to identify possible active or remnant subduction zones is a very important problem. In Taiwan an experiment is now underway (the TAIGER project, see Conclusion) and one of the targets is the upper mantle anomalies.

SEISMICITY

We have already discussed the seismicity associated with the subduction zones in Taiwan and in South Island. The collision zones between the two subductions in these two areas bear interesting comparisons. The earthquake foci in this zone in South Island are concentrated above 25 km [*Davey et al.*, this volume], and probably above 12 km under the high Southern Alps and deeper under lesser topography. The seismicity in central Taiwan, roughly between 23°–24°N – where the collision is most active, is higher than that of South Island, consistent with the higher rate of convergence. In all the profiles of Figure 2c, an overall arch is seen in the seismicity from the Coastal Plain to the high peaks region though there are some gaps in some profiles under the Central Range. In the Coastal Range area, on the PSP side, events down to about 50 km are common but in the Foothills they extend only down to about 35 km. In Figure 2c the Chi-Chi aftershocks are included; *Wu et al.* [2004] compared pre-Chi-Chi and post-Chi-Chi seismicity in detail. Whether pre- or post-Chi-Chi, the boundary between the Foothills and the Central Range is an important one for the seismicity distribution. While the aseismic Central Range is defined by this boundary, so is a steeply west-dipping seismic zone after Chi-Chi (Figure 2c #1 and #2) at depths between 15 and 35 km. A large aftershock occurred in this zone on June 20, 2000. Its own aftershock sequence within 10 hours define a narrow zone and its orientation agrees with the steep plane of it focal mechanism

On the eastern side of the southern part of Central Taiwan (Figure 2c, #5–7) a very clear zone of east-dipping zone of seismicity projects into the LV on land. The larger events along the zone show clear thrust motions (Figure A2 on the CD-ROM which accompanies this volume), providing a mechanism for the Coastal Range to form.

The aftershock seismicity of the M7.6 Chi-Chi earthquake remained high for several years and only began to return to the pre-Chi-Chi level in 2006. The majority of events occurred under the Foothills but around the latitude of 24°N

shallow aftershocks continue across the Central Range. The group of deeper events located from 15–35 km under the boundary between the Foothills and the Central Range mentioned above was unprecedented. As shown by the focal mechanism of a large foreshock in the zone on June 10, 2000, and its own aftershocks within 10 hours of the origin time, the dipping zone is most probably associated with a reverse fault with the Foothills side up and the Central Range side down. This counterintuitive result can be interpreted as a part of the processes that built the Central Range root

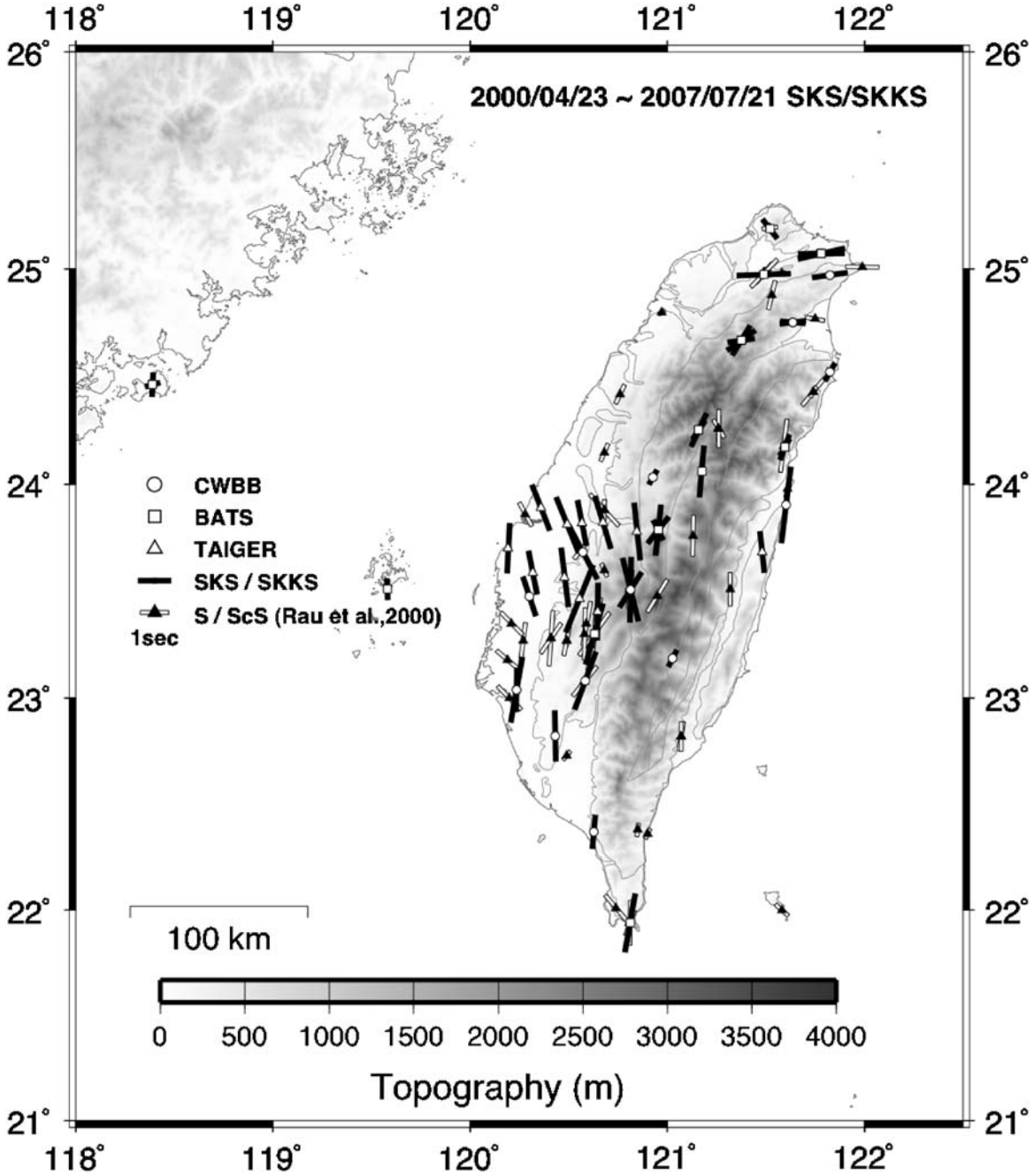

Figure 4. S-splitting results of *Wu et al.* [2007] and *Rau et al.* [2000]. SKS/SKKS data from TAIGER, BATS and CWBB stations are used by Wu et al. and short period CWBSN and BATS data are used by Rau et al. The length of the bar shows the delay time between the fast and slow S-wave and the direction of the bar shows the direction of the fast S-wave.

[*Wu et al.*, 2004]. A full account of the Chi-Chi aftershocks can be found in *Wu et al.* [2004].

S-SPLITTING MEASUREMENTS

Crustal s-splitting

In South Island the schistose crustal rocks are highly anisotropic in laboratory measurements but S-splitting measurements yield delays less than 0.1 sec [see *Savage et al.*, this volume]. In Taiwan a few crustal S-splitting results show similar results [*Kuo et al.*, 1994; *Rau R.J.,* personal communication, 2006]. Recent measurements of schistose rocks in Taiwan indicate large anisotropy of more than 15% [*Christensen*, personal communication, 2007], with the anisotropic axes aligning to the foliation.

Mantle s-splitting

The SKS splitting measurements on South Island were among some of the earlier dataset showing large delay times and the concordance of the fast directions and the surface geological trends [*Klosko et al.*, 1999; *Savage et al.*, this volume: Figure 1]. *Savage et al.* [this volume] summarized the S-splitting results of South Island as well as the North Island. For Taiwan, *Rau et al.* [2002] used S and ScS phases recorded on short-period CWBSN and some broadband BATS stations to determine the splitting parameters. They obtained delay times ranging from 0.5 to 2.1 seconds and found the fast directions to be generally parallel to the trends of local structures (see Figure 4). In northern Taiwan, where the structure turns from NNE to nearly EW, the fast direction of SKS follows it. Using SKS data from one Mozambique event recorded at a line of temporary broadband stations across southern Taiwan and several BATS stations, *Huang et al*. [2006] show a very dramatic increase of delay times in the Central Range – from less than 1 second to more than 2 seconds, with the high values within a distance of about 15 km. Recently *Hao et al*. [2007] added more SKS/SKKS data from several events recorded at BATS as well as temporary stations (the "TAIGER" network) and found a more pervasive trend-parallel pattern. The data around the "Peikang basement high" (Figure 1) is especially clear and the new data also confirmed the fast-direction measurements of *Rau et al.* [2000] in northern Taiwan (Figure 4).

DISCUSSION

The tectonics of South Island and Taiwan are both dominated by a young transpressional collision in a zone between two subduction systems. The history of the evolutionary orogeny in these two regions began more than 5 millions ago. In Taiwan however, an acceleration of the process may have taken place in the past million years. Currently both orogens have about the same physical stature although the strain rate and the erosion mechanisms are different. Taiwan is experiencing much more shortening than South Island although South Island is subjected to more shear. The strain rate calculated from GPS measurements reflects these differences; the areal strain rate of Taiwan is about one order of magnitude greater than that of South Island at 1.5 ppm. The high strain rate in Taiwan may have led to a different mode of deformation, at least at shallow depth: the high Central Range is in a region of dilation in Taiwan but across South Island only compression is observed.

One of the obvious differences between the two orogens is the degree of contrast in the deformation on the two sides of the plate boundary. In South Island the AUS is apparently so rheologically strong that little deformation is found on that side of the Alpine fault. On the other hand, there is considerable shortening of the PSP side to form the Coastal Range in Taiwan. Furthermore, frequent large earthquakes (M6–M7.5) occur on the PSP side and they are known even on the Taiwan Strait side. These earthquakes can be explained by the higher rate of convergence near Taiwan, implying higher stress and strain rates.

The geometry of the colliding and subducting PSP with the EUR east of central and northern Taiwan should affect the deformation on the island. South of the intersection of the Ryukyu Arc with Taiwan, full collision – from surface down to depth – is taking place. But to its north, collision occurs at increasingly greater depth; there the top part of the orogen is no longer in collision and the compression from the collision should be lessened. The expected changes can be seen clearly in Plate 2; north of the Ryukyu intersection the magnitude of the velocities decrease quickly. In southern Taiwan, across the transition from collision to subduction near 23°N, the area should be coupled to the PSP and move westward with it. In Plate 2, a very rapid increase of velocity toward the west and southwest in the Hengchun Peninsula is shown, consistent with the westward motion of PSP over the subducting EUR. In South Island, although the transitions from subduction to collision in the north and the south are sharp in terms of seismicity, the changes in surface deformation in terms of GPS measurements [*Beavan et al.*, this volume: Figures 3 and 4] are much subtler.

One of the most striking similarities of South Island to Taiwan is in the relation between S-splitting parameters and the structural trend of the orogen. The concordance of fast directions with structures is illustrated in South Island and is further affirmed in Taiwan. The wrap-around in the Peikang Basement High in central western Taiwan and the

large clockwise rotation to EW in northern Taiwan are clear with the recent addition of data. The usual argument that the source of the splitting is anisotropy in the upper mantle [*Silver*, 1996] can be applied here and equally applicable is the conclusion that shear strain parallel to the orogen may responsible for the lattice-preferred orientation (LPO) of minerals in the upper mantle. Thus both South Island and Taiwan orogenies may involve vertically coherent deformation through the crust and upper mantle. The EW orientation of fast directions in northern Taiwan is curious in that the region overlies the PSP subduction and the orientation of the PSP fast direction is not known. At the same time, we discussed earlier the westward movement of PSP under Taiwan; it is possible that the flow around the plate or the end of the subduction zone flow may be the cause. We note that away from South Island or Taiwan delay times become small. In the case of Taiwan, the delay times in the Penghu Islands and near the shore of SE China the delays are less

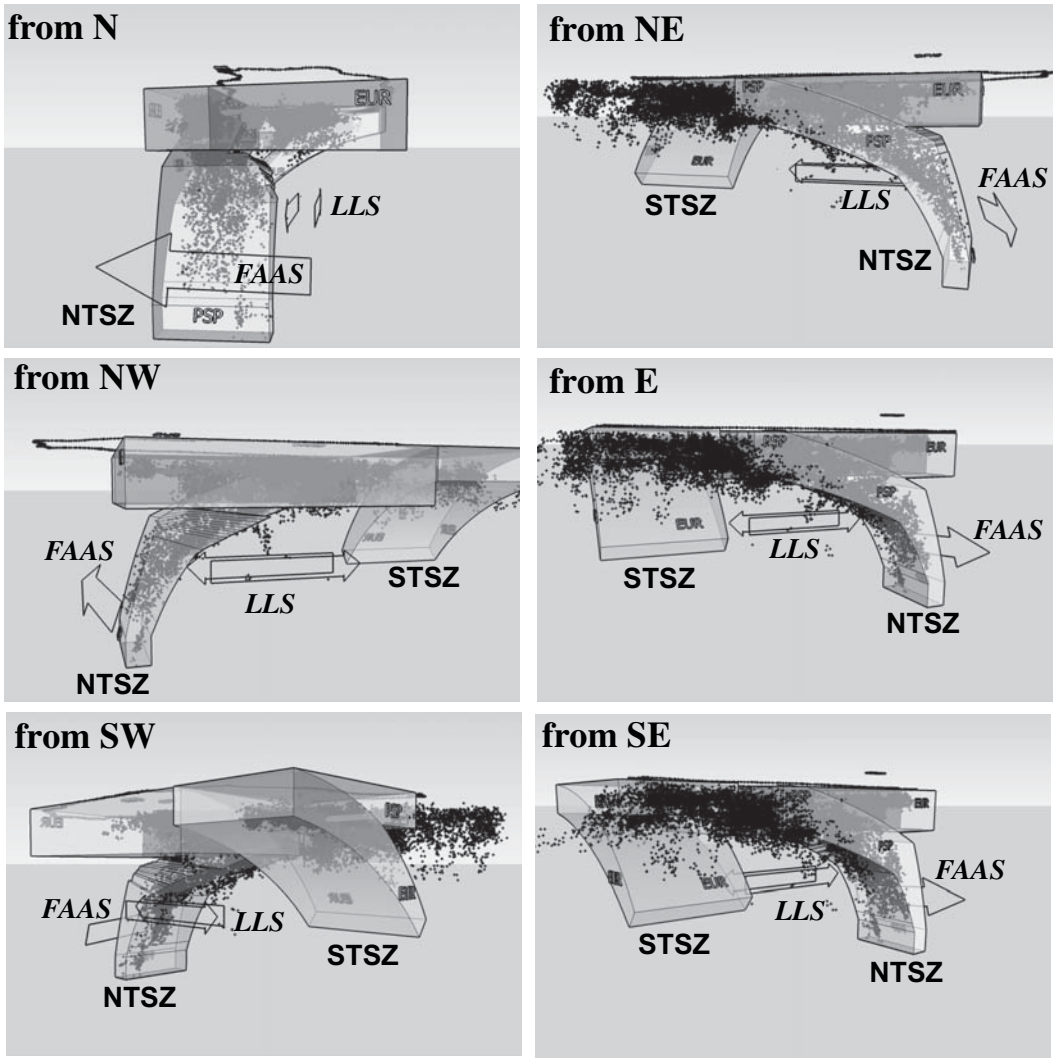

Figure 5. 3D perspectives of plate structures based on seismicity. STSZ=Southern Taiwan subduction zone; NTSZ=Northern Taiwan subduction zone; LLS=Left-lateral shear, shown by a pair of oppositely directed arrows; FAAS=possible upper mantle flow around the westward advancing slab, shown by a single arrow north of the northward subducting PSP. For the different panels: "From N" shows the N-directed subduction zone in frontal view "From NW" shows a side view of the NTSZ and the backside view of STSZ. "From SW" indicates that PSP is overriding EUR as it advances westward. "From NE" and "From E" and "From SE" indicate the subduction of the PSP and a kink in the PSP.

than 0.5 seconds (Figure 4). It would be difficult to explain the large delays on Taiwan if EUR subducts under Taiwan, unless it has an undetected vertical anisotropy or the subducted lithosphere has been subjected to large shear.

Both orogens are already quite mature, having developed a mountain range and a substantial root. The shallowness or absence of seismicity in both ranges argues for relatively high temperature in comparison to surrounding areas. The relatively high velocity in the Central Range [*Rau and Wu*, 1995] (Plate 3a) indicates that mid-crustalal rock under the Central Range may have been uplifted as a result of shortening. In South Island the uplift is achieved mainly through thrusting along the Alpine fault [*Cox and Sutherland*, this volume]. In Taiwan it seems to be accomplished in a broader zone. There is now evidence in Taiwan to show that a high angle reverse fault at depth between the Foothills and the Central Range may be the mechanism for root formation. In other words, pure shear deformation forms the Central Range of Taiwan while simple shear controls the uplift of the Southern Alps.

A summary of the tectonics of Taiwan is presented in Figure 5. The block structures are constructed to surround the seismicity and represent the plate structure. The northern Taiwan subduction zone (NTSZ) is the most prominent structure in the region. Implied in the model is that the subducted PSP is connected to the PSP as a whole and the continued motion of the plate pushes the subducted PSP westward into the mantle. At shallow depth, PSP is shortened to form the Coastal Range (and partially eroded away). Once it enters the region below the lithosphere it starts to move westward and created the curved edge of the NTSZ in the "From N" view. The advancing slab moves the materials in front of it out of the way to form the "flow around advancing slab" or FAAS (Figure 5). This flow could create LPO and may explain the orientation of the fast direction of the S-splitting measurements. In the south, EUR subducts under PSP. However, considering the absolute plate motion (in the no-net-rotation or hot-spot frameworks [*Stein and Wysession*, 2003]), PSP has a rate of 43 cm/yr in the N47°W direction while EUR has a rate of 26 cm/yr in the direction of S70°E, i.e., in the absolute motion framework PSP is overriding EUR. The plate structure seen from the east (in "from NE", "from E" and "from SE" views of Figure 5) indicates the bending of the PSP as it subducts under EUR. The bending of the PSP could be related to the opening of the Okinawa Trough pushing the Ryukyu accretionary wedge southward. The oblique convergence may have also created a shear in the mantle as indicated by the pair of arrows below Taiwan, marked "LLS" or left-lateral shear. In this case, shear is the mechanism that creates the LPO that causes the SKS-splitting.

CONCLUSION

Although the plate tectonic frameworks for both South Island and Taiwan have many similarities, the rates of plate motion and the materials involved in the orogenic processes are different enough to create two different mountain ranges. Under the Central Range of Taiwan pure shear deformation, involving the simultaneous construction of the mountain and the root, is taking place. Dilatation at the earth surface, shown by strain calculations, point to "flowering" of the high mountain range. In South Island simple shear focussed about the Alpine fault built the Southern Alps.

The common observation of large S-splitting delays and the parallelism of the fast-directions with the structural trend are very well illustrated in both regimes. That the source of the splitting resides in the upper mantle seems to be the best hypothesis at present. If the implied vertical coherence [*Molnar et al.*, 1999] is the correct interpretation, then the mountain building processes must involve the crust and upper mantle. Splitting measurements in both Taiwan and South Island are so numerous and robust they provide important constraints to the modeling of orogeny.

The orogenies of Taiwan and South Island have drawn wide attention in the global geosciences community. The SIGHT and SAPSE project in the late 1990's advanced the state of knowledge concerning South Island. In terms of the knowledge regarding crustal and upper mantle structures, South Island is at a much more advanced state than it is in Taiwan. In fact these experiments served as examples for an ongoing project in Taiwan. The Taiwan Integrated Research in Geodynamics (TAIGER) will conduct a series of experiments, including land active source and sea-land transects, and broadband seismic deployment not only on land but also under the ocean. One of the unanswered questions in South Island is the width of the anomalous SKS zone. The TAIGER project will address this problem in Taiwan.

Finally, the accumulated data for both orogens are now quite extensive. Geodynamic modeling constrained by observational data in these two regions will signifcantly advance our understanding of mountain building processes.

Acknowledgements. The authors would like to acknowledge contributions from their colleagues on the SAPSE team. FTW and DO are supported by NSF Continental Dynamics program (NSF EAR-0410227). FD is supported by the NZ Foundation for Research Science and Technology. They would like to dedicate this paper to the memory of Tom McEvilly who was instrumental in organizing SAPSE as a cooperative effort with Helen Anderson. FTW thanks Dr. L.C. Kuo of IES, Academia Sinica for his effort in building an open GPS database. FTW also thanks H. Kuo-Chen for his assistance and Rick Allmendinger for his strain calculation program. Editorial effort by Dr. E. Sonley of SUNY/Binghamton is greatly appreciated.

REFERENCES

Batt, G. E., and J. Braun (1999), The tectonic evolution of the Southern Alps, New Zealand: insights from fully thermally coupled dynamical modeling, *Geophys. J. Int.*, *136*, 403–420.

Beavan, J., S. Ellis, L. Wallace, P. Denys (this volume), Kinematic constraints from GPS on oblique convergence of the Pacific and Australian Plates, central South Island, New Zealand.

Beggs, J. M.; G. A. Challis, and R. A. Cook (1990), Basement geology of the Campbell Plateau; implications for correlation of the Campbell magnetic anomaly system, *N. Z. J. Geol. Geophys., 33*, 401–404.

Carena S., J. Suppe, and H. Kao (2002) - The active detachment of Taiwan illuminated by small earthquakes and its control of first-order topography, *Geology, 30*, 935–938.

Chen, P. F., B. S. Huang, and W. T. Liang (2004), Evidence of a slab of subducted lithosphere beneath central Taiwan from seismic waveforms and travel times, Earth Planet, *Earth Planet. Sci. Lett., 229*, 61–71.

Condie, K. C. (2000), Episodic continental growth models; afterthoughts and extensions, *Tectonophysics*, 322, 153–162.

Cooper, M. R. (1989), The Gondwanic bivalve Pisotrigonia (Family Trigoniidae), with description of a new species, *Palaeontol. Z., 63*, 241–250.

Coward, M. P. (1983), Thrust tectonics, thin skinned or thick skinned, and the continuation of thrusts to deep in the crust, *J. Struct. Geol., 5*, 113–123.

Q2 Coward, M. P. (1996), Balancing sections through inverted basins, in *Modern Developments in Structural Interpretation, Validation and Modelling*, *Soc. Spec. Publ.*, vol. 99, edited by P. G. Buchanan and D. A. Niewland, pp. 51–77.

Cox, S. C., and R. Sutherland (this volume), Regional geological framework of South Island, New Zealand, and its significance for understanding the active plate boundary.

Davey, F., D. Eberhart-Phillips, M. D. Kohler, S. Bannister, G. Caldwell, S. Henrys, M. Scherwath, T. Stern, and H. van Avendonk (this volume), Geophysical structure of the Southern Alps Orogen, South Island, New Zealand.

Davis, G. H., and S. J. Reynolds (1996), *Structural Geology of Rocks and Regions*, John Wiley and Sons, New York.

Davis, D., J. Suppe, and F. A. Dahlen (1983), Mechanics of fold-and-thrust belts and accretionary wedges, *J. Geophys. Res., 88*(B2), 1153–1172.

Eberhart-Phillips, D., and M. E. Reyners (1997), Continental subduction and three-dimensional crustal structure: the northern South Island, New Zealand. *J. Geophys. Res.*, *102*, 11,843–11,861.

Fuller, C. W., S. D. Willett, D. Fisher, and C. Y. Lu (2006), A thermomechanical wedge model of Taiwan constrained by fission-track thermochronometry, *Tectonophysics, 425*, 1–24.

Ho, C. S. (1986), A synthesis of the geologic evolution of Taiwan, *Tectonophysics, 125*, 1–285.

Hu, J.-C., S.-B. Yu, J. Angelier, and H.-T. Chu (2001), Active deformation of Taiwan from GPS measurements and numerical simulations, *J. Geophys. Res.*, *106*, 2265–2280, doi:10.1029/2000JB900196.

Huang, B.-S., W.-G. Huang, W.-T. Liang, R.-J. Rau, and N. Hirata (2006), Anisotropy beneath an active collision orogen of Taiwan: results from across islands array observations, *Geophys. Res. Lett., 33*, L24302, doi:10.1029/2006GL027844.

Huang, C. Y., C. T. Shyu, S. B. Lin, T. Q. Lee, and D. D. Sheu (1992), Marine geology in the arc-continent collision zone off southeastern Taiwan; implications for late Neogene evolution of the Coastal Range, *Mar. Geol., 107*, 183–212.

Kimbrough, D. L., A. J. Tulloch, D. S. Coombs, C. A. Landis, M. R. Johnston, and J. M. Mattinson (1994), Uranium-lead zircon ages from the Median Tectonic Zone, South Island, New Zealand, *N. Z. J. Geol. Geophys., 37*, 393–419.

Kao, H., and P. R. Jian (2001), Seismogenic patterns in the Taiwan region; insights from source parameter inversion of BATS data, *Tectonophysics, 333*, 179–198.

Kim, K. H., J. M. Chiu, J. Pujol, K. C. Chen, B. S. Huang, Y. H. Yeh, and P. Shen (2005), Three-dimensional VP and VS structural models associated with the active subduction and collision tectonics in the Taiwan region, *Geophys. J. Int.*, *162*(1), 204–220. doi:10.1111/j.1365-246X.2005.02657.x

Kuo, B. Y., C. C. Chen, C. C., and Shin, T. C. (1994), Split S waveforms observed in northern Taiwan; implications for crustal anisotropy, *Geophys. Res. Lett., 21*, 1491–1494.

Kuo-chen, H., F. T. Wu, D. A. Okaya, B. S. Huang, and W. T. Liang (2007), *S-Splitting Measurements and Taiwan Orogeny*, AGU Fall Meeting, San Francisco, CA.

Lallemand, S., Y. Font, H. Bijiwaard, and H. Kao (2001), New insights on 3-D plates interaction near Taiwan from tomography and tectonic implications, *Tectonophysics*, 335, 229–253.

Landis, C. A., and D. S. Coombs (1967), Metamorphic belts and orogenesis in southern New Zealand, *Tectonophysics, 4*, 501–518.

Lee, Y. H. (1997), Structural Evolution of Middle Central Range during the Penglai Orogeny, Taiwan, Ph.D. thesis, Institute of Geology, National Taiwan University, Taipei, Taiwan.

Lee, Y. H., C. C. Chen, T. K. Liu, H. C. Ho, H. Y. Lu, and W. Lo (2004), Mountain building mechanisms in the southern Central Range of the Taiwan orogenic belt; from accretionary wedge deformation to arc-continental collision, *Earth Planet. Sci. Letts., 229*, 61–71.

Lee, Y. H., and C. C. Chen (2006), Mountain building mechanisms in the southern Central Range of the Taiwan orogenic belt; from accretionary wedge deformation to arc-continental collision, *Earth Planet. Sci. Letts.*, *252*, 413–422.

Lin C. H., K. I. Konstantinou, W. T. Liang, H. C. Pu, Y. M. Lin, S. H. You, and Y. P. Huang (2006), Preliminary analysis of volcanoseismic signals recorded at the Tatun Volcano Group, northern Taiwan, *Geophys. Res. Lett.,* 32, L10313. doi:10.1029/2005GL022861

Liu, Char-Shine, I. L. Huang, and L. S. Teng (1997), Structural features off southwestern Taiwan, *Marine Geology, 137*, 305–319.

Mikumo T., Y. Yagi, S. K. Singh, and M. A. Santoyo (2002), Coseismic and postseismic stress changes in a subducting plate: possible stress interactions between large interplate thrust and intraplate normal-faulting earthquakes, *J. Geophys. Res.,* 107 (B1), 2023, doi:10.1029/2001JB000446.

McIntosh, K., Y. Nakamura, T.-K. Wang, R.-C. Shih, Allen Chen, and C.-S. Liu (2005), Crustal-scale seismic profiles across Taiwan and the western Philippine Sea, *Tectonophysics,* 401, 23–54.

Mortimer, N., A. J. Tulloch, R. N. Spark, N. W. Walker, E. Ladley, A. Allibone, and D. L. Kimbrough (1999), Overview of the Median Batholith, New Zealand: a new interpretation of the geology of the Median Tectonic Zone and adjacent rocks, *J. African Earth Sci., 29*, 257–268.

Mouthereau, F., and C. Petit (2003), Rheology and strength of the Eurasian continental lithosphere in the foreland of the Taiwan collision belt: constraints from seismicity, flexure, and structural styles, *J. Geophys. Res., 108*, 2512, doi:10.1029/2002JB002098.

Nakamura, M. (2004), Crustal deformation in the central and southern Ryukyu Arc estimated from GPS data, *Earth Planet. Sci. Letts*., *217*, 389–398, doi:10.1016/S0012-821X(03)00604-6

Rau, R.-J., and F. Wu (1995), Tomographic imaging of lithospheric structures under Taiwan, *Earth Planet. Sci. Letts.*, *133*, 517–532.

Rau, R. J., W. T. Liang, H. Kao, and B. S. Huang (2000), Shear wave anisotropy beneath the Taiwan orogen, *Earth Planet. Sci. Letts., 177*, 177–192.

Reed, D. L., N. Lundberg, C. S. Liu, and B. Y. Kuo (1992), Structural relations along the margins of the offshore Taiwan accretionary wedge; implication for accretion and crustal kinematics, *Acta Geologica Taiwanica, 30*, 105–122.

Savage, M., M. Duclos, and K. Marson-Pidgeon (this volume), Seismic anisotropy in South Island, New Zealand.

Sibuet, J. C., and S. K. Hsu (2004), How was Taiwan created?, *Tectonophysics, 379*, 159–181.

Sibuet, J. C., S. K. Hsu, C. T. Shyu, and C. S. Liu (1995), Structural and kinematic evolutions of the Okinawa Trough backarc basin, in *Backarc Basins; Tectonics and Magmatism*, Plenum Press, New York, pp. 343–379.

Silver, P. G. (1996), Seismic anisotropy beneath the continents: probing the depths of geology, *Annu. Rev. Earth Planet. Sci.*, *24*, 385–432.

Stein, S., and M. Wysession (2003), *An Introduction to Seismology, Earthquakes, and Earth Structure*, Blackwell Publishing Ltd., Malden, MA.

Stern, T. A., P. Molnar, D. Okaya, and D. Eberhart-Phillips (2000), Teleseismic P-wave delays and modes of shortening the mantle beneath the South Island, New Zealand, *J. Geophys. Res., 105*, 21,615–21,631.

Stern T., D. Okaya, S. Kleffmann, M. Scherwath, S. Henrys, and F. Davey (this volume), Geophysical exploration and dynamics of the Alpine fault zone.

Suppe, J. (1985), *Principles of Structural Geology*, Prentice-Hall, Englewood Cliffs, NJ, 537 pp.

Suppe, J. (1987), The active Taiwan mountain belt, in *The Anatomy of Mountain Ranges*, Princeton Univ. Press, Princeton, NJ, pp. 277–293.

Tozer, R. S. J., R. W. H. Butler, and S. Corrado (2002), Comparing thin- and thick-skinned thrust tectonic models of the Central Apennines, Italy, EGU, *Stephan Mueller Spec. Publ. Ser.*, *1*, 181–194.

Tulloch, A. J., and D. L. Kimbrough (2003), Paleozoic plutonism in the New Zealand sector of Gondwana, *Geosci. Aust.*, 123–124.

Twiss, R. J., and E. Moores (1992), *Structural Geology*, W. H. Freeman, New York, 532 pp.

Walcott, R. I. (1998), Modes of oblique compression: late Cenozoic tectonics of the South Island, New Zealand, *Rev. Geophys., 36*, 1–26.

Wang. Z., D. Zhao, J. Wang, and H. Kao (2007), Tomographic evidence for the Eurasian lithosphere subducting beneath south Taiwan, *Geophys. Res. Letts., 33*, doi:10.1029/2006GL027166.

Wu, F., R. J. Rau, and D. Salzberg (1997), Taiwan orogeny: thin-skinned or lithospheric collision, *Tectonophysics, 274*, 191–220.

Wu F. T., L. C. Kuo, and H. Kuo-Chen (2007), *Deformation of Taiwan from Continuous GPS Monitoring*, AGU Fall Meeting, San Francisco, CA.

BOOK: **Okaya — GM01075** **CHAPTER 18**

TO: CORRESPONDING AUTHOR

AUTHOR QUERIES - TO BE ANSWERED BY THE AUTHOR

The following queries have arisen during the typesetting of your manuscript. Please answer these queries.

Q1	Please provide Author name(s) and Affiliation(s).
Q2	Please specify if the publisher and it's location.